

INTERNAL CIRCULATING CURRENT IN SYNCHRONOUS GENERATOR AT NO-LOAD AND LOAD CONDITIONS

A. S. Abdallah

Electrical Engineering Department, Assiut University, Assiut, Egypt

ABSTRACT

This paper presents a proper representation of the iron loss in the equivalent circuit of synchronous machines. It is represented by an equivalent core resistance in parallel with a magnetizing reactance, across the machine terminals. Mathematical expressions describing the core resistance and the magnetizing reactance have been derived. Such representation dictates a flow of internal circulating current. The circulating current in the synchronous generator at no-load and various loading conditions has been investigated. The dependency of the circulating current on the field current, terminal voltage and the load angle, is discussed. Moreover, the contributions of the core-loss current component as well as the magnetizing current component to the circulating current are also demonstrated. It is found that the circulating current is as large as 0.032 p.u. at no-load and can reach 0.063 p.u. at maximum loading condition. The circulating current is found to be mainly due to the core-loss current component while the contribution of the magnetizing current component is insignificant. The calculated values of the terminal voltage and the no-load iron loss using the circulating current are found in a good agreement with those measured within errors of $\pm 5\%$ and $\pm 7\%$, respectively.

Keywords: Synchronous machine performance, Equivalent circuit, Iron loss.

INTRODUCTION

Accurate prediction of synchronous machine performance requires proper representation of the iron loss in their modeling. In this context, the prediction and simulation of the iron loss has been the subject of many investigators [1-11]. In References 8 to 11, a qualitative study of the iron loss has been carried out. In other investigations [3-5], the distribution of the iron loss inside the machine has been assessed. Others [1-5, 7-9] investigated the loading effect on the iron loss. In Reference 2 an approximate representation of the iron loss in the equivalent circuit of synchronous machines has been suggested. No attempt was made to predict the "so-called internal circulating current" that causes the iron loss inside the machine.

This paper presents a proper representation of the iron loss in the equivalent circuit of synchronous machines. The internal circulating current at no-load and different loading conditions has been investigated. To check the calculated values of the internal circulating current, the no-load iron loss and the machine open circuit voltage are calculated using the corresponding circulating current and the calculated values are compared with those measured experimentally. The agreement between the calculated and measured values is satisfactorily within an error not exceeding 7% confirming the accuracy of the calculated circulating current values. The internal circulating current increases with the increase of the load angle. For the investigated machine, it could be as large as 6.3%.

SYNCHRONOUS MACHINE EQUIVALENT CIRCUIT

First of all, the magnetic saturation of the synchronous machine has been represented by replacing the unsaturated values of the d- and q-axis synchronous reactances x_{mdu} and x_{mqu} with their saturated values x_{mds} and x_{mqs} [12]. The details of this method are reported in the Appendix.

Then, the synchronous machine has been represented by an emf E_{fs} in series with an equivalent impedance Z_{eq} [2]. A phasor diagram showing this equivalent circuit is shown in Figure 1.

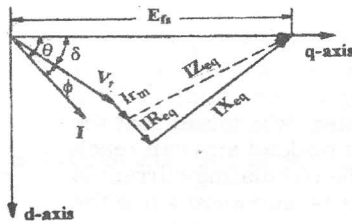


Figure 1 Phasor diagram of the equivalent circuit of a synchronous generator.

The terminal voltage \bar{V}_t has been expressed in terms of the excitation voltage \bar{E}_{fs} and the equivalent impedance, \bar{Z}_{eq} as follows:

$$\bar{V}_t = \bar{E}_{fs} - \bar{I} R_{eq} - j \bar{I} X_{eq} \tag{1}$$

where

$$\bar{E}_{fs} = X_{mds} I_f \tag{2}$$

$$\bar{Z}_{eq} = R_{eq} - j X_{eq} \tag{3}$$

$$R_{eq} = \frac{X_{ds} - X_{qs}}{2} \sin 2\theta \tag{4}$$

$$X_{eq} = \frac{X_{ds} - X_{qs}}{2} - \frac{X_{ds} + X_{qs}}{2} \cos 2\theta \tag{5}$$

where R_{eq} and X_{eq} are the machine equivalent resistance and reactance. θ is the internal power factor angle.

PROPER REREPRESENTATION OF THE IRON LOSS

Recently, the iron loss components P_{cq} and P_{cd} due to the d- and q-axis ampere-turns have been measured experimentally in a specially designed synchronous generator. The method of measuring these iron loss

components is reported in Reference 1. Also, mathematical expressions describing the iron loss components P_{cq} and P_{cd} have been formulated as follows [1]:

$$P_{cq} = \frac{V_q^2}{R_{cq}} \tag{6}$$

$$P_{cd} = \frac{V_d^2}{R_{cd}} \tag{7}$$

where V_d and V_q are the terminal voltage components on the d- and q-axis. R_{cd} and R_{cq} are the iron resistance along the d- and q-axis paths.

Equation 6 and 7 can be rewritten as follows:

$$P_{cq} = I_{cq} V_q \tag{8}$$

$$P_{cd} = I_{cd} V_d \tag{9}$$

where I_{cd} and I_{cq} are core-loss current components on the d- and q-axis respectively. I_{cd} and I_{cq} can be expressed in terms of the terminal voltage V_t and the load angle δ , as follows:

$$I_{cd} = \frac{V_d}{R_{cd}} = \frac{|V_t| \sin \delta}{R_{cd}} \tag{10}$$

$$I_{cq} = \frac{V_q}{R_{cq}} = \frac{|V_t| \cos \delta}{R_{cq}} \tag{11}$$

Combining Equations 10 and 11, the total core-loss current I_c can be obtained as follows:

$$\bar{I}_c = I_{cq} - j I_{cd} \tag{12}$$

$$\bar{I}_c = \frac{|V_t| \cos \delta}{R_{cq}} - j \frac{|V_t| \sin \delta}{R_{cd}} \tag{13}$$

Equation 13 can be rewritten as follows:

$$\bar{I}_c = \bar{V}_t \left(\cos \delta - j \sin \delta \right) \left(\frac{\cos \delta}{R_{cq}} - j \frac{\sin \delta}{R_{cd}} \right) \tag{14}$$

Equation 14 can be rewritten in the following form:

$$\bar{I}_c = \bar{Y}_{eq} \bar{V}_t \tag{15}$$

where \bar{Y}_{eq} is the core equivalent admittance and can be written in the following formula:

$$\bar{Y}_{eq} = \frac{R_{cd} + (R_{cq} - R_{cd}) \sin^2 \delta}{R_{cd} R_{cq}} - j \frac{(R_{cq} - R_{cd}) \sin 2\delta}{2 R_{cd} R_{cq}} \quad (16)$$

Equation 16 can be rewritten as follows:

$$\bar{Y}_{eq} = \frac{1}{R_c} - j \frac{1}{X_c} \quad (17)$$

where R_c is a resistance representing core losses and X_c is a reactance representing some leakage flux in stator core. R_c and X_c can be expressed as follows:

$$R_c = \frac{R_{cd} R_{cq}}{R_{cd} + (R_{cq} - R_{cd}) \sin^2 \delta} \quad (18)$$

$$X_c = \frac{2 R_{cd} R_{cq}}{(R_{cq} - R_{cd}) \sin 2\delta} \quad (19)$$

From Equations 1, 15 and 17, a proper representation of the iron loss in the equivalent-circuit of synchronous machines is achieved as shown in Figure 2. It is quite clear that the internal circulating current I_c has two components, Figure 2, namely a loss current component I_{ca} and a magnetizing component I_{cr} .

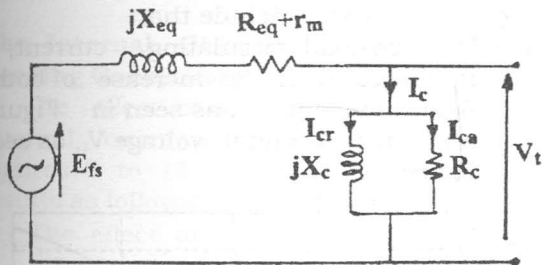


Figure 2 Equivalent circuit of a synchronous machine including iron loss representation.

RESULTS AND DISCUSSION

The equivalent circuit shown in Figure 2 has been used for investigating the internal circulating current I_c at no-load and various loading conditions. The description and parameters of the investigated synchronous generator are given in the Appendix.

Characteristics of the Core Resistance and Magnetizing Reactance

The dependency of the core resistance, R_c , and the magnetizing reactance X_c on the load angle, δ , is shown in Figures 3 and 4. Moreover, the variations of R_c and X_c with the output active power, P , at different values of the reactive output power, Q , can be also obtained. The method of calculation is given in the Appendix. The variations of R_c and X_c with P and Q are shown in Figures 5 and 6. From these figures, one can conclude:

i - Figure 3 shows that the core resistance, R_c decreases with the increase of the load angle, δ , or the output active power, P . At load angle $\delta = 0$, $R_c = R_{cq}$ and at load angle $\delta = 90^\circ$, the core resistance $R_c = R_{cd}$.

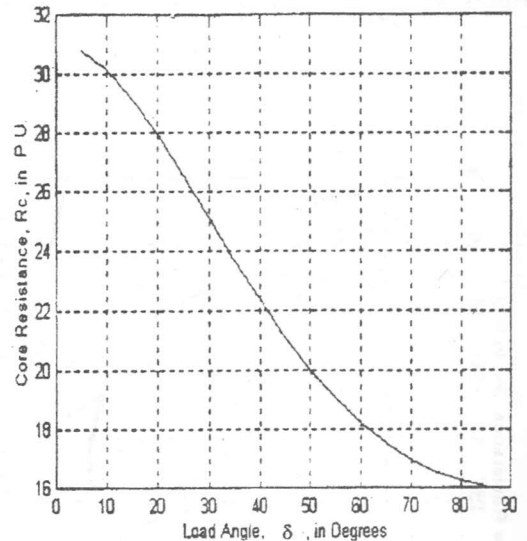


Figure 3 Variation of the core resistance, R_c , against the load angle, δ , at $V_t = 1.0$ p.u. and $I_f = 1.0$ p.u.

- ii- Figure 5 shows that the core resistance, R_c , decreases also as the power factor varies from lagging to leading.
- iii- The magnetizing reactance, X_c , has a minimum value at load angle $\delta = 45^\circ$ and increases by changing the load angle δ beyond this value, as seen in Figure 4.
- iv- The magnetizing reactance, X_c , decreases with the increase of the output active power, P . It decreases also by changing the power factor from lagging to leading, as seen in Figure 6.

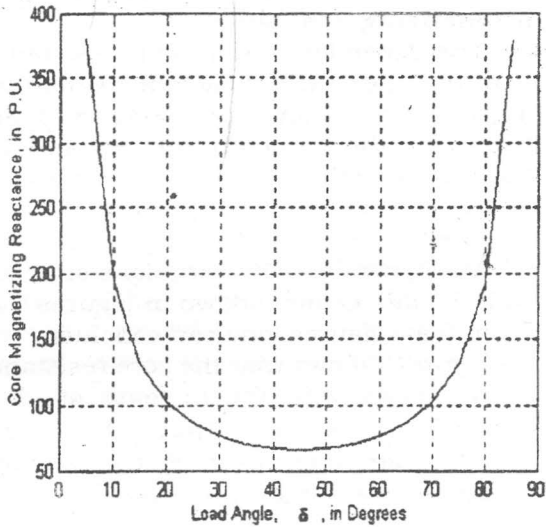


Figure 4 Variation of the core magnetizing reactance, X_c , with the load angle, δ , at $V_t = 1.0$ p.u. and $I_f = 1.0$ p.u.

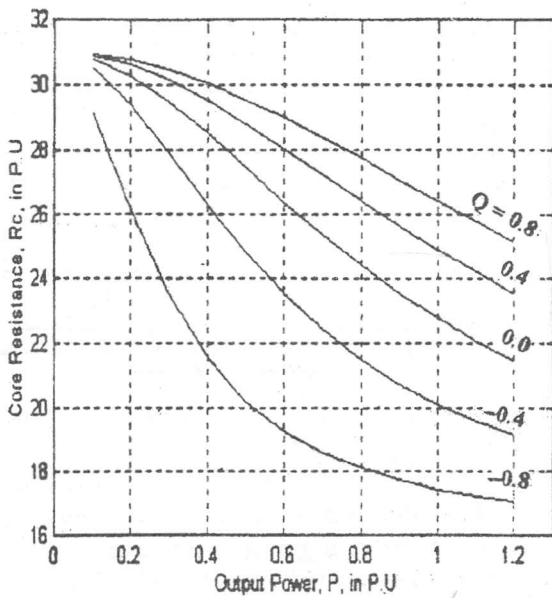


Figure 5 Variation of the core resistance, R_c , with the output active power, P , at different values of the output reactive power, Q , and $V_t = 1.0$ p.u.

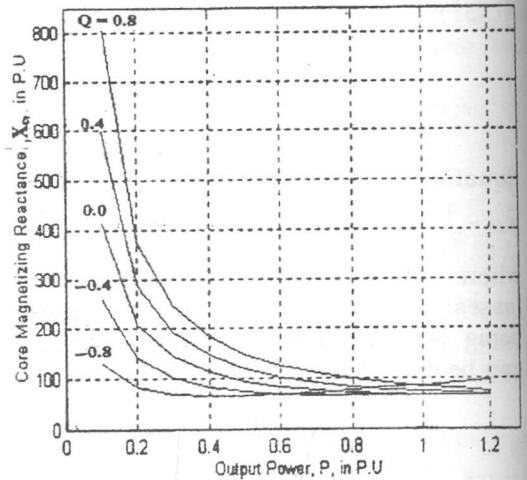


Figure 6 Variation of the magnetizing reactance, X_c , with the output active power, P , at different values of the output reactive power, Q , and $V_t = 1.0$ p.u.

The Internal Circulating Current At No-Load Condition

Figures 7 and 8 show the effect of field current and terminal voltage on the no-load circulating current, I_c . Moreover, the contributions of the current components I_{ca} and I_{cr} to the no-load current, I_c , are also shown in the same figures. From these figures, one can conclude that:

- i - The no-load circulating current, I_c , increases with the increase of both the field current I_f , as seen in Figure 7, and the terminal voltage V_t , as seen in Figure 8.

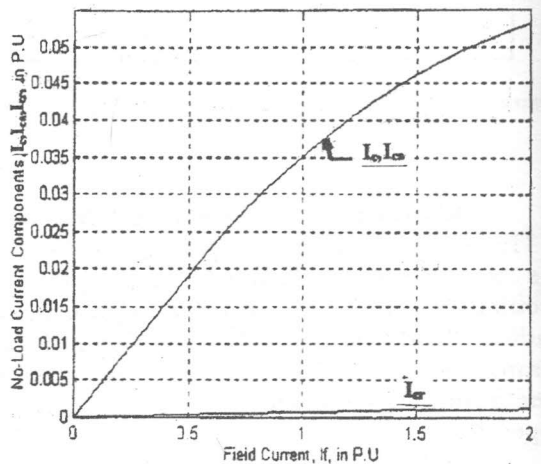


Figure 7 Variation of the no load current components, I_c , I_{ca} , I_{cr} with the field current I_f .

- ii - Figure 8 shows that for the investigated synchronous generator, the no-load current, I_c , could be as large as 0.032 p.u. at rated voltage
- iii- The no-load current, I_c , is mainly due to the current loss component, I_{ca} , and the contribution of the magnetizing current component, I_{cr} , to the no-load circulating current, I_c , is negligible, as seen from figures 7 and 8.

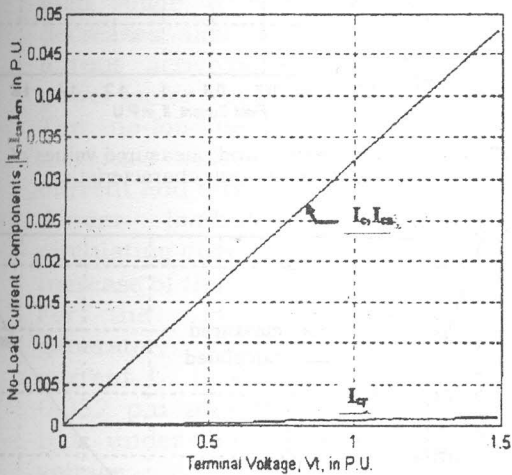


Figure 8 Variation of the no load current components, I_c , I_{ca} , I_{cr} with the terminal voltage V_t .

The Internal Circulating Current Under Loading Conditions

The effect of loading conditions on the internal circulating current is shown in Figures 9 to 11. It is worthy to discuss the results as follows:

- i - The effect of the load angle, δ , on the internal circulating current I_c and its components I_{ca} and I_{cr} is shown in Figure 9. It is quite clear that the internal circulating current I_c increases with the increase of the load angle, δ . For the investigated synchronous generator, this current I_c could be as large as 0.063 p.u. at rated voltage and load angle $\delta = 90^\circ$. the internal current I_c depends mainly on the current loss component I_{ca} , Figure 9. Shows that The maximum contribution of the core magnetizing current I_{cr} is 0.015 p.u. at a load angle $\delta = 45^\circ$.

- ii- Figure 10 shows the effect of the load angle, δ , on the power factor angle, ϕ_c , of the internal circulating current which is defined as the angle between the current I_c and the terminal voltage V_t . For the investigated synchronous generator, the angle ϕ_c has a constant value of 1.4° at no-load. With loading the generator the angle ϕ_c has a maximum value of 18.5° at a load angle $\delta = 35^\circ$.
- iii- Figure 11 shows the effect of the load angle, δ , and the terminal voltage, V_t , on the internal circulating current I_c . The internal circulating current I_c increases with the increase of either the terminal voltage, V_t , or the load angle δ .

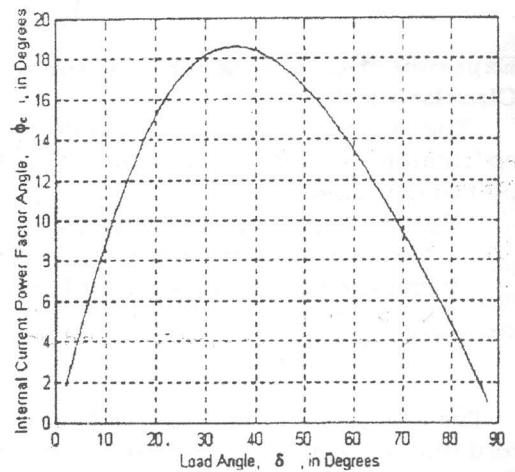


Figure 9 Variation of the circulating current components, I_c , I_{ca} , I_{cr} with the load angle δ , at $V_t = 1$ p.u.

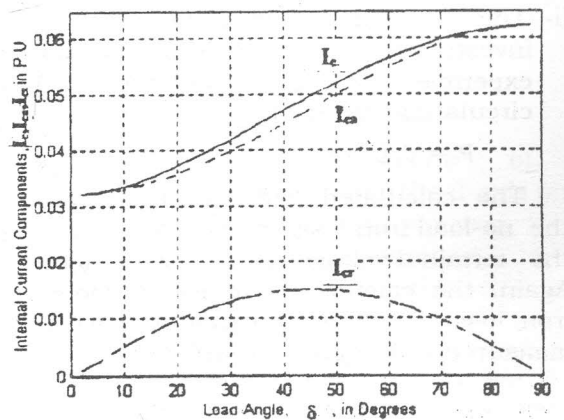


Figure 10 Variation of the internal power factor angle, ϕ_c , with the load angle δ .

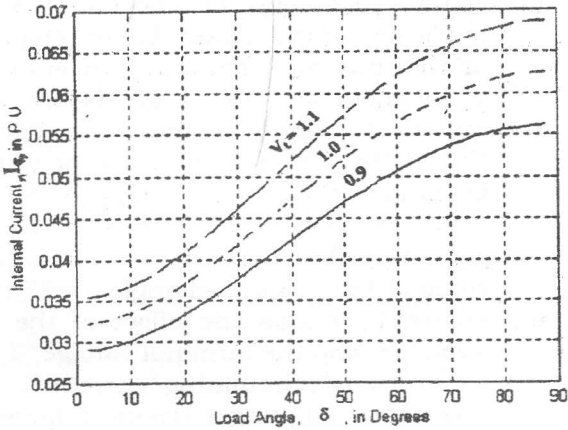


Figure 11 Variation of the circulating current I_c , with the load angle δ , at different values of the terminal voltage, V_t

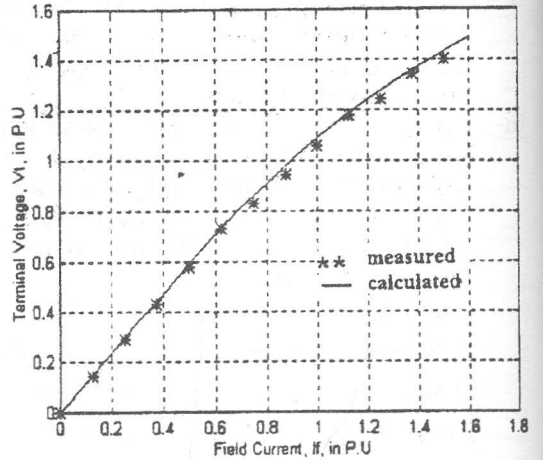


Figure 12 Calculated and measured values of the d-axis open-circuit characteristic.

Experimental Check-Up of the Internal Circulating Current

The accuracy of the calculated internal circulating current, I_c , has been checked-up by two methods:

- i - The machine open-circuit voltage was measured experimentally and calculated using the circulating current I_c as:

$$V_t = \frac{I_c}{Y_{eq}} \quad (20)$$

The calculated and measured values of the terminal voltage, V_t , at different values of the field current, I_f are shown in Figure 12. It is satisfactory to observe the agreement of the calculated values of the terminal voltage with those measured within an error of 5%.

- ii- The no-load iron loss, P_c , of the investigated generator was also measured experimentally and calculated using the circulating current I_c as:

$$P_c = V_t I_c \cos \phi_c \quad (21)$$

The calculated and measured values of the no-load iron loss, P_c , at different values of the terminal voltage are shown in Figure 13. Again, the calculated values of the no-load iron loss, P_c agreed satisfactorily with those measured within an error of 7%.

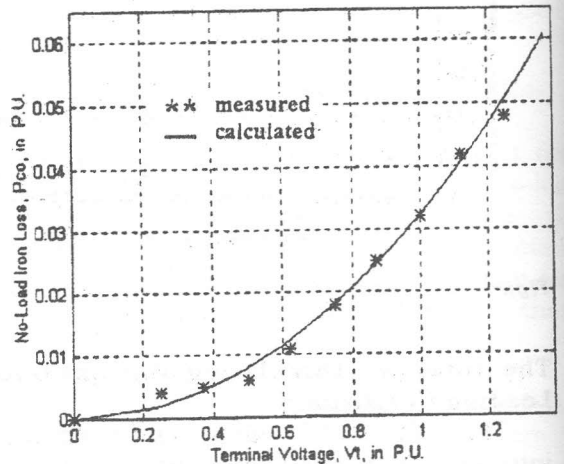


Figure 13 Calculated and measured values of the no-load iron loss, P_{co} , against the terminal voltage, V_t .

CONCLUSIONS

The iron loss has been represented in the equivalent circuit of synchronous machines by a core resistance, R_c , parallel to a magnetizing reactance, X_c , across the machine terminals. Mathematical expressions describing the core resistance as well as the magnetizing reactance have been derived. The internal circulating current, I_c , in synchronous generator at no-load as well as at different loading conditions has been investigated. The contributions of the current loss component, I_{ca} , and the magnetizing current component, I_{cr} , to the internal circulating current, I_c , at no-load as well as

various loading conditions are also demonstrated. From this study, one can conclude:

- i- The core resistance, R_c , decreases with the increase of the load angle, δ , or the output active power. It decreases also with the change of the power factor from lagging to leading.
- ii- The magnetizing reactance, X_c , has a minimum value at load angle $\delta = 45^\circ$ and increases with the change of the load angle δ beyond this value. It decreases also with the increase of the output active power or by changing the power factor from lagging to leading.
- iii- The no-loading circulating current I_c , increases with the increase of the field current and terminal voltage.
- iv- Under loading condition, the internal circulating current I_c , increases with the increase of the load angle, δ .
- v. For the investigated synchronous generator, the internal circulating current I_c , is found to be as large as 0.032 p.u at no-load and up to 0.063 p.u under loading condition at rated voltage.
- vi. The internal circulating current I_c , is found to be mainly due to the current loss component, I_{ca} , and the contribution of the magnetizing current component, I_{cr} , to the internal circulating current, I_c , is found to be negligible at no-load and up to 0.015 p.u. under loading condition.
- vii - The angle φ_c , between the current I_c , and the terminal voltage varies with the load angle δ . For the investigated synchronous generator, this angle φ_c , has constant value of 1.4° at no-load and varies up to 18.5° under loading condition.
- viii- As a check for the accuracy of the calculated circulating current, the calculated values of the terminal voltage using the circulating current I_c , are found in a good agreement with the measured results within an error of 5%. Also, the calculated values of the no-load iron loss using the circulating current I_c , are found to be in a good

agreement with their measured results within an error of 7%.

APPENDIX

Representation of the Magnetic Saturation

In Reference 12, the magnetic saturation of synchronous machines has been represented in the conventional d- and q-axis frame model by replacing the unsaturated values of the machine reactances with their saturated values. The saturated values of the d- and q-axis mutual reactances, $X_{m_{ds}}$ and $X_{m_{qs}}$, could be obtained by modifying their unsaturated values $X_{m_{du}}$ and $X_{m_{qu}}$ by using two d- and q-axis saturation factors in addition to the cross-magnetizing effect. The equations describing the saturated reactances are given as follows:

$$X_{m_{ds}} = S_d X_{m_{du}} \cdot \frac{\Psi_{dq}}{AT_d} \quad (A-1)$$

$$X_{m_{qs}} = S_q X_{m_{qu}} \cdot \frac{\Psi_{qd}}{AT_q} \quad (A-2)$$

where S_d and S_q are the d- and q-axis saturation factors. They could be obtained from the machine d- and q-axis open-circuit characteristic curves. For the synchronous machine under investigation, the equations describing the saturation factors S_d and S_q are given as follows [13]:

$$S_d = \begin{cases} 1.0 & |AT_d| \leq AT_{ds} \\ 1.0 - \alpha_d (AT_d - AT_{ds}) & |AT_d| > AT_{ds} \end{cases} \quad (A-3)$$

$$S_q = \begin{cases} 1.0 & |AT_q| \leq AT_{qs} \\ 1.0 - \alpha_q (AT_q - AT_{qs}) & |AT_q| > AT_{qs} \end{cases} \quad (A-4)$$

where:

AT_d is the component of the ampere-turns in the d-axis and is equal to $|I_f - I_d|$ in per unit,

AT_q is the component of the ampere-turns in the q-axis and is equal to $|I_q|$ in per unit,

AT_{ds}, AT_{qs} are the absolute values of the ampere-turns at which the d- and q-axis open-circuit characteristics start to be non-linear, respectively,

α_d, α_q are constants representing the steepnesses of the open-circuit characteristics in the d- and q-axis respectively,
 I_d, I_q are the d- and q-axis components of the armature current, respectively, in per unit,
 I_f is the field winding current in per unit,
 Ψ_{dq}, Ψ_{qd} are the changes in the d- and q-axis flux linkages due to the cross-magnetizing effect. In Reference 13 both Ψ_{dq} and Ψ_{qd} are measured experimentally under loading conditions in the form of two d- and q-axis voltage drops E_{qd} and E_{dq} . For the synchronous machine used in the investigations reported in this paper, the equations describing Ψ_{dq} and Ψ_{qd} are given as follows [13]:

$$\Psi_{qd} = \begin{cases} 0.0 & |AT_d| \leq C_{od} \\ \gamma_{dq} AT_q (AT_d - C_{od}) & |AT_d| > C_{od} \end{cases} \quad (A-5)$$

$$\Psi_{dq} = \begin{cases} 0.0 & |AT_q| \leq C_{cq} \\ \gamma_{qd} AT_d (AT_q - C_{cq}) & |AT_q| > C_{cq} \end{cases} \quad (A-6)$$

where $\gamma_{dq}, \gamma_{qd}, C_{od}, C_{cq}$ are constants.

The Machine Used For Studies

The machine used for the studies is a small salient-pole machine. It has wound rotor windings on both its d- and q-axis. It is a 4-pole machine and its nominal ratings are as follows: 3 KVA, 220/127 V, 60Hz, 1800 rpm. The machine parameters used in the paper are given in Table A-1.

Table A-1 The Machine Parameters

The machine parameters	The values in p.u.	The machine parameters	The values in p.u.
Xmdu	1.189	Cod	0.312
Xmqd	0.716	Coq	0.265
Xla	0.091	Rcd	16.0
α_d	0.223	Rcq	31.0
α_q	0.104	γ_{dq}	0.260
ATds	0.624	γ_{qd}	0.160
ATqs	0.530		

Calculation Of R_c And X_c Versus P And Q

For a given output active power P, reactive power Q and terminal voltage V_t the load angle δ can be obtained for unsaturated synchronous machine as follows:

$$\phi = \tan^{-1} \frac{Q}{P} \quad (A-7)$$

$$I = \frac{P}{V_t \cos \phi} \quad (A-8)$$

$$\delta = \tan^{-1} \frac{IX_q \cos \phi - I r_m \sin \phi}{V_t - I r_m \cos \phi + IX_q \sin \phi} \quad (A-9)$$

Substituting from Equation A-9 in Equations 18 and 19, the values of R_c and X_c can be obtained. In the case of saturated synchronous machine, the value of X_q Equation A-9 will be replaced by its saturated value X_{qs} as reported in Reference 12 and described in the first part of the Appendix. The value of load angle δ can be obtained through an iterative procedure using Equations A-1 to A-6 in addition to Equation A-7 to A-9. Subsequently, the variations of R_c and X_c with P and Q can be obtained using Equations 18 and 19.

REFERENCES

1. A. S. Abdallah, "Effect of Loading Conditions on the Iron Loss in Synchronous Machines", A paper Accepted for publication in the Bulletin of the Faculty of Engineering Assiut University, (1999).
2. A. S. Abdallah, "A Simplified Equivalent circuit of Synchronous Machines Including Saliency, Saturation and Core Losses", Bulletin of the Faculty of Engineering, Assiut University, Vol. 20, Part 2, July pp. 51-57, (1992)
3. H. C. Karmaker, "Stray Losses in large Synchronous Machines", IEEE Trans. on Energy Conversion, Vol. 7, No. 1, pp. 148-153, (1992)
4. H. C. Karmaker, "Synchronous Machines Losses", Proceedings of the International Conference on Electrical Machines, ICEM'90, Cambridge, Massachusetts, August 13-15, USA, Vol. 2, pp. 378-383, (1990)

5. H. Ohishi, "Calculation of No Load Loss and Stray Load Loss", Proceedings of the International Conference on Electrical Machines, ICEM'84, (1984)
6. IEEE Guide, "Test Procedures for Synchronous Machines", IEEE Standards 115-(1983)
7. H. C. Karmaker, "Open Circuit Tooth Ripple Losses in Slotted Laminated Poles of Electrical Machines with Amortisseur Windings", IEEE Trans, PAS-101, May pp. 1122-1128, (1982)
8. R. L. Winchester, "Stray Losses in the Armature End Region of Large Turbine-Generators", AIEE Trans., Vol. 74, pt. III, pp. 381-391, (1955)
9. P. Richardson, " Stray Losses in Synchronous Electrical Machinery", IEE Journal, Vol. 92, pp. 312-315, (1945)
10. E. I. Pollard, "Calculation of No-Load Damper Winding Loss in Synchronous Machines", AIEE Trans., pp. 477-482, (1932).
11. C. M. Laffoon, and J.F. Calvert, "Iron Losses in Turbine Generators", AIEE Trans. Vol. 48, pp. 370-374, (1929).
12. A. M. El-Serafi and A. S. Abdallah, "Synchronous Reactances of Saturated Synchronous Machines", IEEE Trans. on Energy Conversion, Vol. 7, No. 3, pp. 570-579, (1992).
13. A. M. El-Serafi and A. S. Abdallah, M. K. El-Sherbiny and E. H. Badawy, "Experimental Study of the Saturation and the Cross - Magnetizing Phenomenon in Saturated Synchronous Machines", IEEE Trans. on Energy Conversion, Vol. EC-3, No. 4, pp. 815-823, (1988)

Received May 3, 1999
Accepted August 16, 1999

تيارات تدور في دورة داخلية بالمولدات الكهربائية المترامنة في حالات اللاحمل والحمل

أحمد سيد عبد الله

قسم الهندسة الكهربائية - جامعة اسيوط

ملخص البحث:

في هذا البحث تم عمل تمثيل دقيق للمفاقيد الحديدية بالدائرة المكافئة للآلات الكهربائية المترامنة . فقد تم تمثيلها بمقاومة قلب توازي مع ممانعة مغنطة توصلان عبر أطراف المولد . وتم إستنتاج صيغ رياضية مناسبة لمقاومة القلب وممانعة المغنطة . وهذا التمثيل للمفاقيد الحديدية أوضح مرور تيار داخلي بالمولدات الكهربائية المترامنة في حالات اللاحمل والحمل . وتم إستنتاج صيغ رياضية للتيار الداخلي ومركباته وهما تيار القلب وتيار المغنطة . وتم دراسة تأثير كل من تيار الإثارة للماكينة والجهد على أطرافها وزاوية الحمل على قيمة التيار الداخلي ومركباته . وأظهرت الدراسة أن قيمة التيار الداخلي في المولد تحت الدراسة في حالة اللاحمل تصل إلى ٣٢٪ وفي حالة الحمل الأقصى تصل إلى ٦٣٪ . وقد وجد أن قيمة التيار الداخلي تعتمد بصورة أساسية على مركبة تيار القلب . أما مشاركة مركبة تيار المغنطة في قيمة التيار الداخلي فقد وجدت ضعيفة . وللتأكد من دقة حساب التيار الداخلي فقد تم إستخدامه في حساب كل من الجهد على أطراف الماكينة والمفاقيد الحديدية في حالة اللاحمل ، وقد وجدت أنهما يتفقان مع القيم المناظرة لهما والمقاسة معمليا وأن نسبة الخطأ في الجهد لا تتعدى $\pm 5\%$ وفي حالة المفاقيد الحديدية لا تتعدى $\pm 7\%$.